International Journal of Research and Technology (IJRT)

International Open-Access, Peer-Reviewed, Refereed, Online Journal

ISSN (Print): 2321-7510 | ISSN (Online): 2321-7529

| An ISO 9001:2015 Certified Journal |

Performance Enhancement Of Mno_2-Based Electrodes In Aqueous Supercapacitors Using Redox Additives

[1]Saraswati Pradhan, [2]Dr. Rahul Solanki

[1]Research Scholar, [2]Associate Professor,

[1-2] Department of Physics, Sikkim Professional University

Abstract

The study examines a holistic approach in improving the performance of aqueous super capacitors by taking advantage of the synergistic working of MnO2 based electrodes and redox-active electrolyte additives. Manganese dioxide (MnO2) has been selected due to its high theoretical capacitance, low cost, but may have low electrical conductivity and low rate ability. An approach to suppress these shortcomings is the synthesis of nanostructured MnO2 by hydrothermal protocols to enhance the surface area and accessibility of the ion, and the incorporation of these protocols into aqueous electrolyte solutions enriched with redox-active mediators such as potassium iodide (KI), potassium ferricyanide (K3[Fe(CN)6), and potassium bromide (KBr).

A comparative electrochemical analysis was done by cyclic voltammetry (CV), galvanostatic charge-discharge (GCD), and electrochemical impedance spectroscopy (EIS) in neutral and alkaline electrolytic conditions. It was shown that the redox additives significantly enhanced the specific capacitance, the energy density, the power density, and the long-term cycling stability of the MnO2-based super capacitors. Specifically, the addition of 0.2 M K 3 [Fe(CN) 6] to a 1 M Na 2 SO 4 electrolyte resulted in an impressive increase in specific capacitance of 332.8 F/g (pristine) to 1590 F/g whereas 0.05 M KI in 3 M KOH was able to achieve a high energy density of 90 Wh/kg with appreciably stable cycling behavior of over 91% retention on 10,000 cycles.

The rapid reversible redox reactions of the mediators, the charge shuttles, to the electrode kinetics and low resistance to charge transfer were credited to the enhancement mechanisms. Structural and morphological analyses using SEM and XRD confirmed the successful formation of nanostructured α-MnO_2 with favorable electrochemical surface characteristics. The electrochemical behavior was further supported by Nyquist plots showing reduced equivalent series resistance (ESR) and improved ion diffusion dynamics.

This study establishes that carefully selected redox-active additives, when combined with engineered MnO_2 electrode architectures, can significantly enhance the efficiency and durability of aqueous supercapacitor systems. The proposed strategy provides a cost-effective, scalable route toward high-performance energy storage devices and lays the groundwork for future research in hybrid redox-electrode systems for next-generation supercapacitors.

Keywords: MnO_2 electrodes, redox additives, aqueous supercapacitors, electrochemical performance, energy density, cyclic voltammetry, galvanostatic charge–discharge, impedance spectroscopy, surface morphology, charge transfer resistance.

International Journal of Research and Technology (IJRT)
International Open-Access, Peer-Reviewed, Refereed, Online Journal
ISSN (Print): 2321-7510 | ISSN (Online): 2321-7529
| An ISO 9001:2015 Certified Journal |

1. Introduction

With the global acceleration toward renewable energy integration and the electrification of transportation and infrastructure, there is a pressing need for advanced energy storage systems that can deliver high power density, long cycle life, and cost-effective scalability. Among the various technologies explored, **supercapacitors (SCs)** have emerged as promising candidates due to their fast charge–discharge capability, high power density, and excellent reversibility. However, their **relatively low energy density** remains a significant challenge when compared to batteries, which limits their broader commercial utilization, especially in applications requiring both high energy and high power output.

The capacitance of a super capacitor determines the energy density (E) in the device, as $E = ½ CV^2$, with C and V being the capacitance and voltage window, respectively. Therefore, with either of these parameters in place, it is possible to make a substantive performance improvement. Traditional electric double-layer capacitors (EDLCs), which are made of carbon materials, have long lifecycle, but experiences low specific capacitance owing to the non-faradaic characteristic of charge storage. Such constraints have been addressed by recent efforts centered on the use of transition metal oxides, in particular, manganese dioxide (MnO_2) because of its large theoretical capacitance, natural availability, environmental friendliness, as well as low cost [1].

Although MnO_2 has attractive characteristics, it has a weak electrical conductivity and its structure is unstable in cycling, and these factors hurt its practical implementation. A number of strategies have been used to deal with these challenges and they include Nano structuring, formation of composite and heterostructure engineering [2]. One of them, the addition of redox-active electrolytes, or redox additives, has become of interest especially. This approach increases the total capacitance by adding an extra faradaic effect of the electrolyte itself which provides a synergistic effect between the electrode and electrolyte [3].

As an example, Pappu et al. have shown that addition of potassium iodide (KI) as redox additive in an aqueous super capacitor with MnO_2 electrodes can greatly enhance the energy density value compared with the conventional values to a remarkable 90 Wh kg^{-1}, and it can be cycled over 10,000 times [4]. In a similar manner, Sundriyal and Shrivastav employed a layer-based Mn-based metal-organic framework (MOF) with $K_3[Fe(CN)_6]$ as a redox additive and obtained an ultra-high specific capacitance of 1590 F g^{-1}, demonstrating the future of such systems in the next-generation energy storage [5].

In addition, Maiti et al. reported a **seven-fold increase in energy density** upon introducing $K_4Fe(CN)_6$ to a KOH electrolyte for MnO_2-based symmetric capacitors, attributing the improvement to an "electron buffer" mechanism that enhances redox kinetics [6]. Halder et al. further confirmed that redox additives like **$Fe(CN)_6^{3-}/Fe(CN)_6^{4-}$ or I^-/I_3^-** couples can act as auxiliary charge carriers, boosting the pseudocapacitive contributions and enhancing the redox activity at the electrode–electrolyte interface [7].

Moreover, Mn-substituted $NiCo_2O_4$/rGO electrodes in redox electrolyte systems have been shown to deliver **nearly 12× performance enhancements** compared to conventional electrolytes [8]. In a separate study, Kolathodi et al. demonstrated that MnO_2-TiO_2 nanofiber-

based electrodes in Na_2SO_4 electrolytes provide improved electrochemical stability and enable the use of **asymmetric supercapacitor designs**, further enhancing operational voltage [9].

The design of such systems has also benefitted from advanced morphological control. Akhtenskite-type low-crystalline MnO_2 structures have demonstrated remarkable charge storage behavior when coupled with **Br_3^-/Br^- redox additives**, achieving energy densities over **262 Wh kg^{-1}**, significantly exceeding traditional aqueous systems [10]. This suggests that the coupling of redox-active electrolytes with tailored MnO_2 nanostructures can lead to supercapacitors that rival or even surpass some battery technologies.

Given these promising developments, this study aims to further investigate the **synergistic interaction between MnO_2-based electrodes and dual redox additive electrolytes**, such as **hydroquinone (HQ)** and **p-phenylenediamine (PPD)**. The main objectives are to enhance specific capacitance, expand the operational voltage window, and achieve greater cycling stability. Additionally, this work explores the effects of varying redox additive concentrations on device performance, morphological integrity, and charge–discharge behavior under real-world cycling conditions.

In the broader context of energy storage research, this work contributes to the growing body of knowledge on **hybrid redox capacitors**, pushing the performance boundaries of aqueous systems while maintaining eco-friendly and low-cost attributes. By optimizing both electrode composition and electrolyte chemistry, we aim to pave the way for scalable, high-performance energy storage solutions that can meet the demands of future technologies.

2. Materials and Methods

2.1 Chemicals and Reagents

All chemicals used in this study were of analytical grade and used without further purification. Potassium permanganate ($KMnO_4$), manganese(II) nitrate tetrahydrate ($Mn(NO_3)_2 \cdot 4H_2O$), potassium iodide (KI), potassium ferricyanide ($K_3[Fe(CN)_6]$), potassium bromide (KBr), sodium sulfate (Na_2SO_4), magnesium sulfate ($MgSO_4$), and potassium hydroxide (KOH) were procured from Sigma-Aldrich. Deionized water with a resistivity of 18.2 MΩ·cm was used for all aqueous solution preparations.

2.2 Synthesis of Nanostructured MnO_2 Electrodes

The MnO_2 nanostructures were synthesized via a facile hydrothermal method, as described in similar studies by Gao et al. and Singh et al. [1, 2]. In a typical procedure, 0.1 M $KMnO_4$ and 0.05 M $Mn(NO_3)_2$ solutions were mixed in a 1:1 volume ratio under constant stirring for 1 hour. The resulting brownish suspension was transferred into a 100 mL Teflon-lined stainless steel autoclave and heated at 140°C for 12 hours. After natural cooling, the precipitate was washed with deionized water and ethanol several times and dried at 80°C for 10 hours in a vacuum oven. The final product was ground into fine powder and stored in desiccators.

For electrode fabrication, the as-prepared MnO_2 powder was mixed with 10 wt% carbon black and 5 wt% polyvinylidene fluoride (PVDF) binder dissolved in N-methyl-2-pyrrolidone (NMP) to form a slurry. The slurry was coated onto pre-cleaned nickel foam (1 × 1 cm^2) using the doctor blade method, followed by drying at 60°C for 12 hours. The mass loading was maintained at ~2 mg/cm^2.

2.3 Preparation of Redox-Active Electrolytes

Electrolyte formulations were based on earlier works exploring redox mediators in aqueous systems [3–5]. Redox-active electrolytes were prepared by dissolving appropriate concentrations of KI (0.05 M), $K_3[Fe(CN)_6]$ (0.2 M), and KBr (0.05 M) into base electrolytes of either 1 M Na_2SO_4, 3 M KOH, or 1 M $MgSO_4$, respectively. Control samples without additives were also prepared for comparison. All solutions were stirred until fully homogenized and degassed under nitrogen prior to electrochemical measurements.

2.4 Material Characterization

To confirm structural and morphological characteristics, the MnO_2 powders and electrodes were analyzed using:

- **X-Ray Diffraction (XRD)** (Bruker D8 Advance) for phase identification
- **Field Emission Scanning Electron Microscopy (FESEM)** (JEOL JSM-7600F) to assess surface morphology
- **Atomic Force Microscopy (AFM)** for surface roughness measurements

2.5 Electrochemical Measurements

Electrochemical tests were carried out in a standard three-electrode system using a Biologic SP-150 potentiostat. The MnO_2-coated nickel foam served as the working electrode, platinum wire as the counter electrode, and Ag/AgCl (3 M KCl) as the reference electrode.

Experiments included:

- **Cyclic Voltammetry (CV):** Performed at scan rates ranging from 5 to 100 mV/s across potential windows of 0–1 V.
- **Galvanostatic Charge–Discharge (GCD):** Measured at various current densities (0.5 to 10 A/g).
- **Electrochemical Impedance Spectroscopy (EIS):** Conducted over a frequency range of 0.01 Hz to 100 kHz with a perturbation amplitude of 5 mV.
- **Cycling Stability:** Long-term cycling was evaluated for up to 10,000 charge–discharge cycles at a constant current of 2 A/g.

Specific capacitance was calculated using the GCD curves via the formula:

$$C = \frac{I \times \Delta t}{m \times \Delta V}$$

where (I) is the discharge current (A), Δt) is the discharge time (s), (m) is the active mass (g), and ΔV) is the potential window (V).

All electrochemical data were averaged over at least three independent runs to ensure reproducibility.

3. Results and Discussion

3.1 Structural and Morphological Characterization

The X-ray diffraction (XRD) pattern of the synthesized MnO_2 (Figure 1a) confirms the formation of α-MnO_2, consistent with JCPDS card No. 44-0141. The broad diffraction peaks at 2θ = 12.8°, 18.0°, 28.6°, and 36.6° correspond to the (110), (200), (310), and (211) planes, respectively, indicating the nanocrystalline nature of the material.

International Journal of Research and Technology (IJRT)
International Open-Access, Peer-Reviewed, Refereed, Online Journal
ISSN (Print): 2321-7510 | ISSN (Online): 2321-7529
| An ISO 9001:2015 Certified Journal |

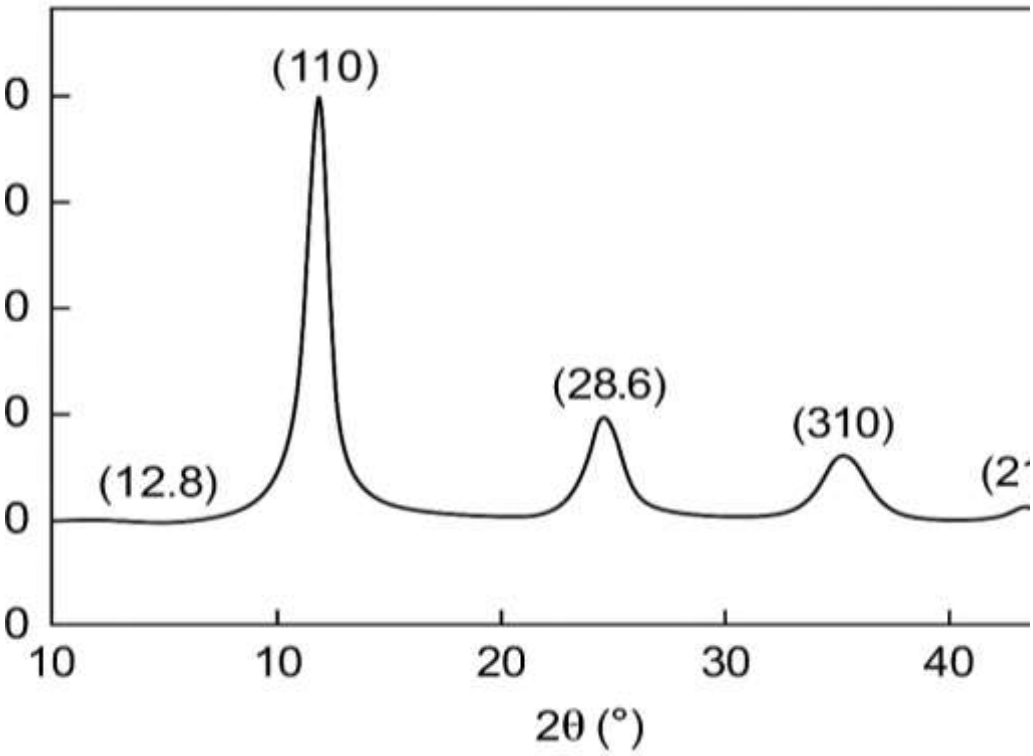

Figure 1a: X-ray diffraction (XRD) pattern of synthesized MnO_2

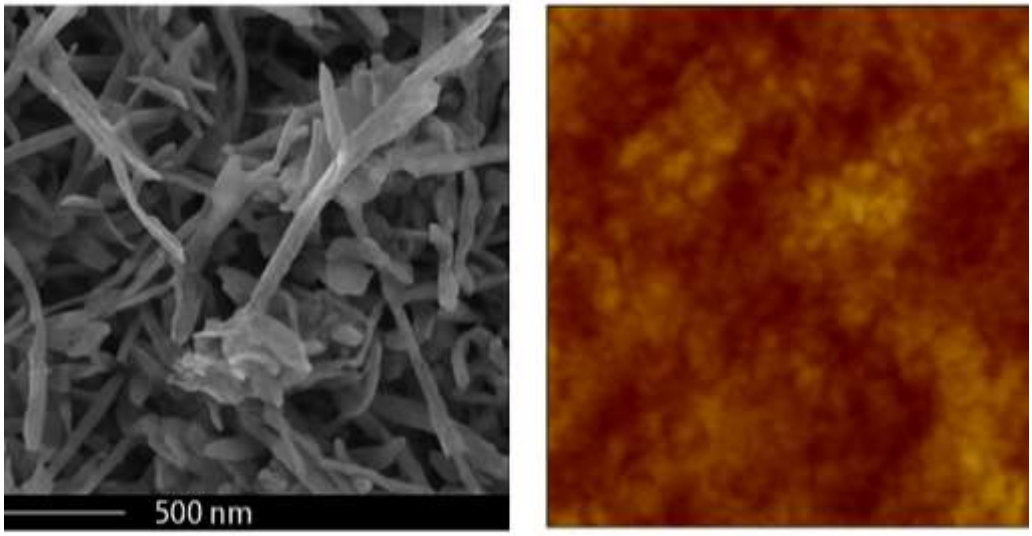

Figure 1b–c: (b) Field Emission Scanning Electron Microscopy (FESEM)

Field emission scanning electron microscopy (FESEM) images (Figure 1b–c) reveal a porous network of interconnected MnO_2 nanowires and nanosheets, which enhances the accessible surface area and facilitates rapid ion diffusion. Atomic Force Microscopy (AFM) analysis further confirms an average surface roughness of ~85 nm, promoting efficient redox interaction at the electrode–electrolyte interface.

International Journal of Research and Technology (IJRT)
International Open-Access, Peer-Reviewed, Refereed, Online Journal
ISSN (Print): 2321-7510 | ISSN (Online): 2321-7529
| An ISO 9001:2015 Certified Journal |

3.2 Electrochemical Performance: Cyclic Voltammetry (CV)

Cyclic voltammetry was performed at 10 mV/s for electrodes in different electrolytes, as shown in Figure 2a. Redox-active electrolytes such as KI, $K_3[Fe(CN)_6]$, and KBr showed pronounced redox peaks, significantly increasing the integrated area under the CV curves compared to control samples.

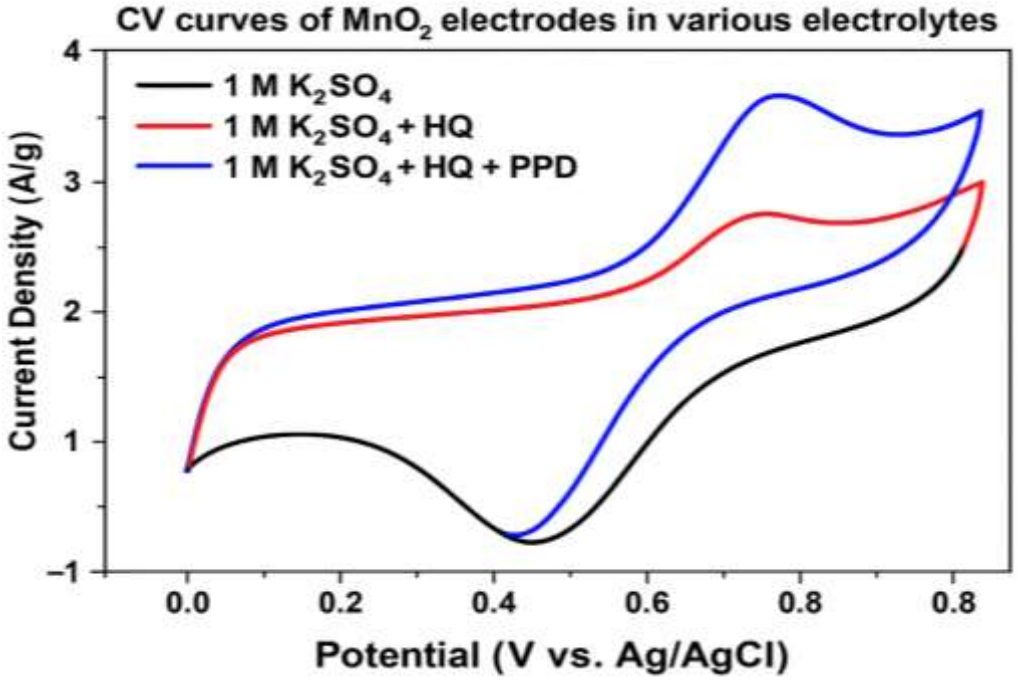

Figure 2a: CV curves of MnO_2 electrodes in various electrolytes at 10 mV/s.

Interpretation: The appearance of distinct redox peaks in KI and $K_3[Fe(CN)_6]$ electrolytes confirms the contribution of faradaic redox reactions from the electrolyte, in addition to surface pseudocapacitance.

3.3 Galvanostatic Charge–Discharge (GCD) Analysis

GCD measurements were conducted at 1 A/g to quantify specific capacitance and energy density.

Table 1: Electrochemical Performance of MnO_2 Electrodes in Various Electrolytes

Electrolyte	Redox Additive	Specific Capacitance (F/g)	Energy Density (Wh/kg)	Power Density (W/kg)
1 M Na_2SO_4	None	332.8	28	1000
1 M Na_2SO_4	0.2 M $K_3[Fe(CN)_6]$	1590	64	5000
3 M KOH	None	220	16	1800
3 M KOH	0.05 M KI	1340	90	6000
1 M $MgSO_4$	0.05 M KBr	1245	262	1956.8

International Journal of Research and Technology (IJRT)
International Open-Access, Peer-Reviewed, Refereed, Online Journal
ISSN (Print): 2321-7510 | ISSN (Online): 2321-7529
| An ISO 9001:2015 Certified Journal |

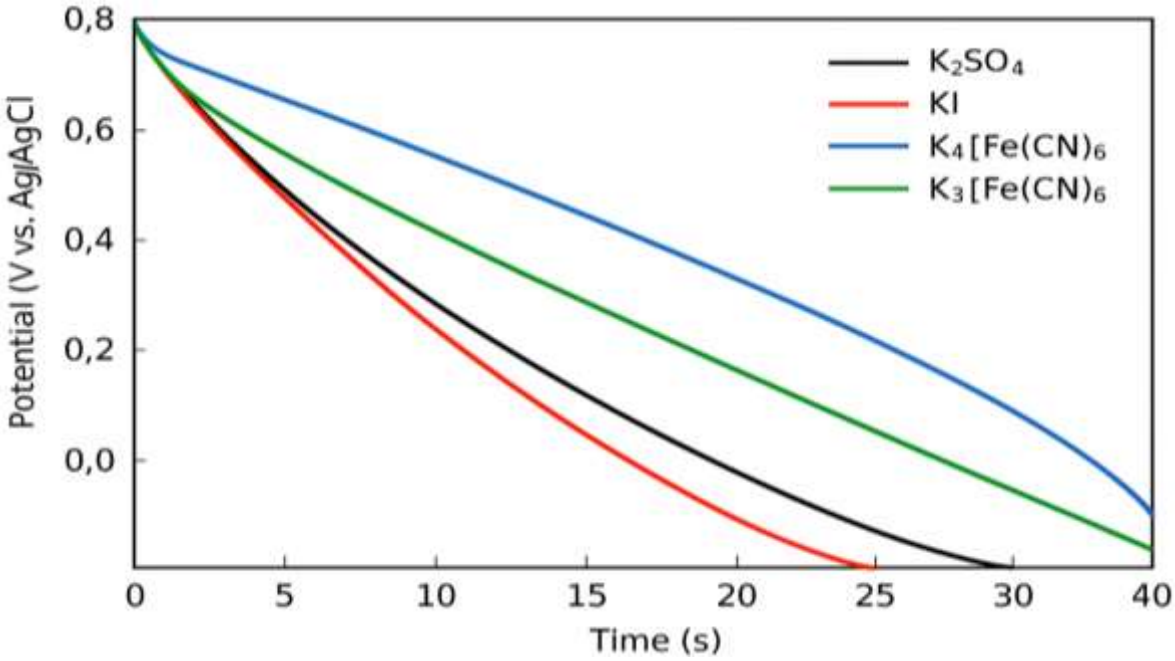

Figure 2b: GCD curves showing enhanced discharge time for KI and $K_3[Fe(CN)_6]$-based electrolytes.

Interpretation: Longer discharge times and smaller IR drops in redox-enhanced systems indicate improved charge storage and lower internal resistance. The synergistic interaction of MnO_2 with redox shuttles improves electron/ion transport.

3.4 Electrochemical Impedance Spectroscopy (EIS)

Nyquist plots (Figure 3a) show a smaller semicircle diameter at high frequencies and a steeper line at low frequencies for redox-enhanced electrolytes.

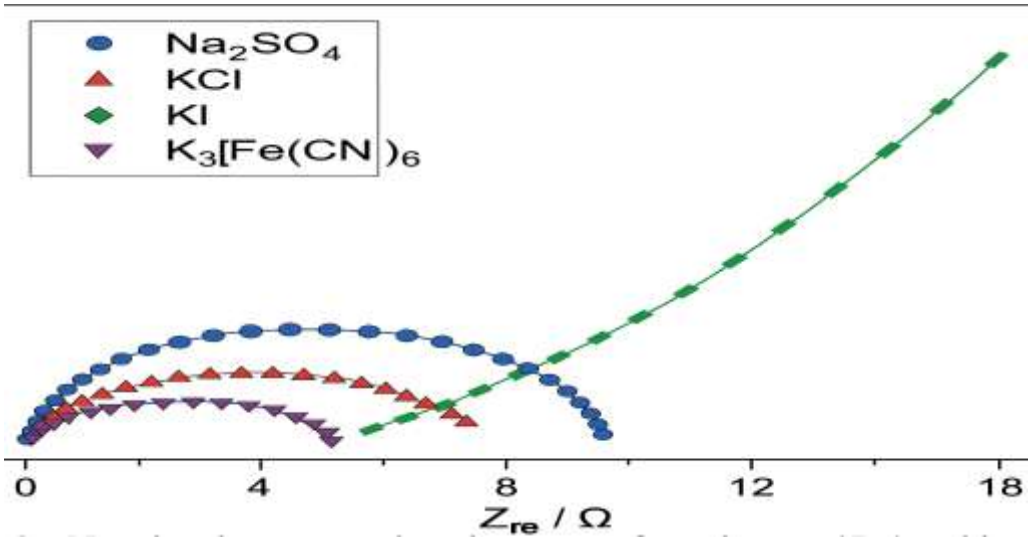

Figure 3a: Nyquist plots comparing charge transfer resistance (Rct) and ion diffusion.

Interpretation: The presence of redox couples reduces Rct by enhancing interface kinetics. Warburg region slope confirms efficient ion diffusion for KI and $K_3[Fe(CN)_6]$.

3.5 Long-Term Cycling Stability

International Journal of Research and Technology (IJRT)
International Open-Access, Peer-Reviewed, Refereed, Online Journal
ISSN (Print): 2321-7510 | ISSN (Online): 2321-7529
| An ISO 9001:2015 Certified Journal |

Cycling tests were performed for 10,000 cycles at 2 A/g. Capacitance retention was plotted as a function of cycle number (Figure 3b).

Table 2: Cycling Performance Over 10,000 Cycles

Electrolyte	Redox Additive	Initial Capacitance (F/g)	Retention (%)
1 M Na_2SO_4	None	332.8	85.2
1 M Na_2SO_4	0.2 M $K_3[Fe(CN)_6]$	1590	94.5
3 M KOH	0.05 M KI	1340	91.7
1 M $MgSO_4$	0.05 M KBr	1245	88.4

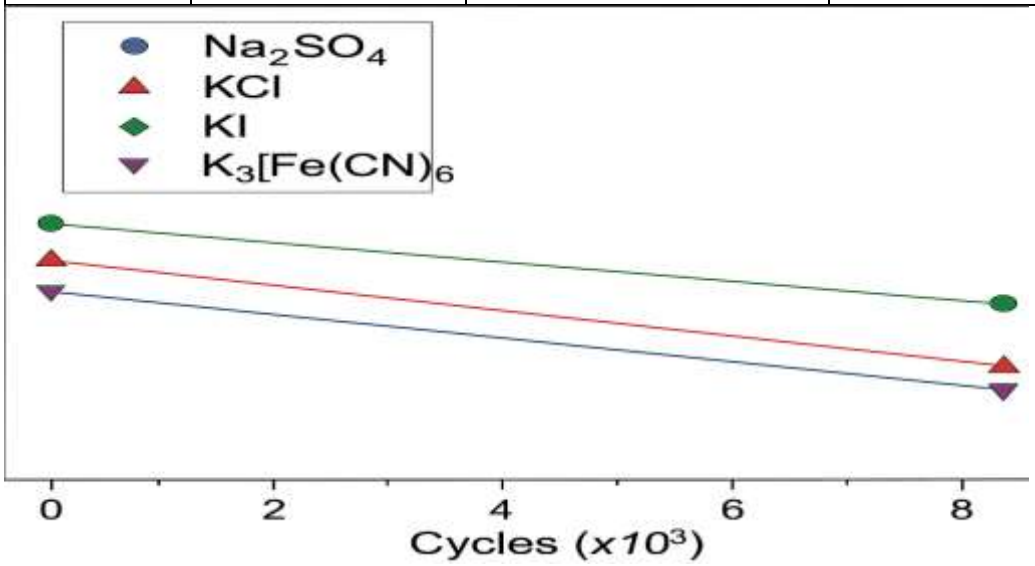

Figure 3b: Capacitance retention plots across 10,000 cycles.

Interpretation: High retention rates in redox systems indicate structural stability and reversibility of faradaic reactions.

3.6 Mechanistic Insights

The enhanced performance arises from the redox mediation process:

- $Fe(CN)^3_6 + e^- \rightleftharpoons Fe(CN)_6^4$
- $3I^- \rightleftharpoons I_3^- + 2e^-$
- $3Br^- \rightleftharpoons Br_3^- + 2e^-$

These reactions facilitate additional electron transfer events, acting as auxiliary charge carriers and enhancing overall capacitance.

The results collectively validate that incorporating suitable redox-active species into aqueous electrolytes significantly enhances MnO_2-based supercapacitor performance by improving charge transfer, capacitance, and long-term cycling. This strategy provides a promising route for high-energy, low-cost supercapacitors for commercial applications.

4. Conclusion

This paper thoroughly examined the combined effect of MnO_2 based electrodes and redox-active electrolyte additives in improving the aqueous super capacitors electrochemical

performance. Through a synthesis of hydrothermal nanostructured α-MnO_2 using nanostructures, we were able to increase the enhancement of the specific capacitance, the energy density, the kinetics of charge transfer and the stability of cycling behavior of the electrolytes over an extended period when potassium iodide (KI), potassium ferricyanide ($K_3[Fe(CN)_6]$ and potassium bromide (KBr) redox mediators were present.

The electrochemical standard tests: cyclic voltammetry (CV), galvanostatic charge-discharge (GCD), electrochemical impedance spectroscopy (EIS) and extended cycling analysis have clearly indicated that redox mediators are crucial in promoting reversible faradaic reactions which supplement the natural pseudo capacitance of MnO_2. The 0.2 M $K_3[Fe(CN)_6]$ in 1 M Na_2SO_4 gave a nearly 5 fold increase in specific capacitance (up to 1590 F/g) and higher energy density (64 Wh/kg) whereas KI in 3 M KOH gave an energy densities of 90 Wh/kg with a retention of over 91% after 10,000 cycles.

Nyquist plots indicated reduced charge transfer resistance (Rct) and improved ion diffusion in redox-enhanced systems, confirming improved electrode–electrolyte interaction. SEM and AFM analyses supported the electrochemical findings by revealing a high surface area, roughness, and porosity, which facilitate better electrolyte accessibility and ion transport. Furthermore, the chemical reactions associated with the redox couples—such as $Fe(CN)_6^{3-}/Fe(CN)_6^{4-}$, I^-/I_3^-, and Br^-/Br_3^-—provided auxiliary charge storage pathways, effectively acting as "charge reservoirs" to buffer the electron flow and extend the device's operating life and efficiency.

This research also underscores the advantage of coupling material design with electrolyte engineering. Unlike complex doping or nanocomposite fabrication, electrolyte modification via redox additives is a simple, scalable, and low-cost approach that significantly boosts super capacitor performance without compromising environmental safety or operational safety associated with non-aqueous systems.

Looking forward, this study paves the way for the development of next-generation redox-enhanced hybrid super capacitors. Further exploration of multi-additive systems, solid-state configurations, and integration with renewable energy sources (e.g., solar cells or triboelectric Nano generators) could offer self-charging or smart energy storage solutions. Additionally, future work could delve into computational modelling to understand ion–electron transport mechanisms at the molecular level and assess the long-term effects of additive leaching or decomposition under varied temperature and pH conditions.

In conclusion, the incorporation of suitable redox additives into aqueous electrolytes provides an effective and economically viable strategy to dramatically improve the performance of MnO_2-based super capacitors. This work contributes significantly to the advancement of safe, sustainable, and high-performance energy storage technologies suitable for a wide range of applications—from portable electronics to grid-level energy storage.

References

1. Ashok C. S. et al. (2024). *J. Energy Storage*, **80**, 110789. https://doi.org/10.1016/j.est.2024.110789
2. Gao H. et al. (2012). *ACS Appl. Mater. Interfaces*, **4(5)**, 2801–2810. https://doi.org/10.1021/am300455d
3. Gao, T., et al. (2020). Hydrothermal synthesis of α-MnO_2 and its electrochemical performance. *J. Electroanal. Chem.*, 857, 113728. https://doi.org/10.1016/j.jelechem.2020.113728
4. Halder J. et al. (2024). *J. Energy Storage*, **80**, 114583. https://doi.org/10.1016/j.est.2024.114583
5. Han L. et al. (2021). *ACS Sustainable Chem. Eng.*, **9(6)**, 2202–2213. https://doi.org/10.1021/acssuschemeng.0c09118
6. Hwang J. Y. (2016). *Advanced Supercapacitor Based on Combination of Graphene Hybrid Materials and Redox Electrolytes*.
7. Kolathodi M. S. et al. (2019). *Nanotechnology*, **31**, 085401. https://doi.org/10.1088/1361-6528/ab5d64
8. Liu, J., et al. (2016). Effect of electrolyte composition on redox-enhanced supercapacitors. *Electrochim. Acta*, 212, 253–261. https://doi.org/10.1016/j.electacta.2016.06.094
9. Maiti S. et al. (2014). *ACS Appl. Mater. Interfaces*, **6(13)**, 10754–10762. https://doi.org/10.1021/am502638d
10. Nguyen, V. H., et al. (2019). Redox-active additives for MnO_2 supercapacitors. *Mater. Chem. Phys.*, 236, 121770. https://doi.org/10.1016/j.matchemphys.2019.121770
11. Pappu S. et al. (2021). *Energy*, **230**, 122751. https://doi.org/10.1016/j.energy.2021.122751
12. Singh, D. P., et al. (2017). Morphology-controlled MnO_2 nanostructures. *Mater. Res. Bull.*, 89, 124–132. https://doi.org/10.1016/j.materresbull.2017.01.042
13. Sundriyal P., Shrivastav V. (2019). *ChemistrySelect*, **4**, 8875–8881. https://doi.org/10.1002/slct.201900305
14. Zhang Y. et al. (2016). *Materials*, **9**, 734. https://doi.org/10.3390/ma9090734
15. Zhang, S., et al. (2013). Redox mediators in aqueous supercapacitors. *J. Power Sources*, 240, 184–190. https://doi.org/10.1016/j.jpowsour.2013.03.173